

## RESEARCH PAPER

## EFFECT OF COLD DEFORMATION AND ANNEALING PHENOMENA ON THE MICROSTRUCTURAL CHANGES AND MICRO-HARDNESS IN Al-Mg-Si ALUMINIUM ALLOYS

Abdelouahab Noua<sup>1,2</sup>, Meryem Guemini<sup>1,2</sup>, Toufik Ziar<sup>2,3\*</sup>, Hichem Farh<sup>2,3</sup>, Rebai Guemini<sup>1,2</sup><sup>1</sup> Department of Material Sciences, Faculty of Exact Sciences, Larbi Ben M'hidi University of Oum El Bouaghi, Algeria.<sup>2</sup> Active devices and material laboratory (LCAM), Larbi Ben M'hidi University of Oum El Bouaghi, Algeria.<sup>3</sup> Department of Material Sciences, Faculty of Exact Sciences, Larbi Tebessi University of Tebessa, Algeria.

\*Corresponding author: toufik1\_ziar@yahoo.fr; Tel.: +213662584466; Fax: +213 03242354. Department of Material Sciences, Faculty of Exact Sciences, Larbi Tebessi University of Tebessa, 12000, Algeria.

Received: 27.06.2020

Accepted: 29.06.2020

**ABSTRACT**

Aluminium alloys are of particular interest because of their low density, low cost and ease of thermo-mechanical processing. During the recent years, much interest has been shown in the development of alloys with optimal mechanical properties which can be retained at high temperatures. The purpose of the present investigation is to study the microstructure of two Al-Mg-Si alloys containing transition elements after cold deformation 10%, 20 %, 30%, 40% and 50% reduction in thickness and annealing at 1 hour at different temperature by using the optical microscopy, transmission electron microscopic (TEM), Vickers hardness measurement. We notice that the micro-hardness increases with the increasing of the deformation level. The coarse particles, with a particle size of about 2 to 3  $\mu\text{m}$ , give rise to a heavily local deformation of the Aluminium matrix. The formation of well-defined substructure due to the arrangement of dislocations is observed after an increase in annealing temperature.

**Keywords:** Al-Mg-Si alloys; Dispersoid particles; Cold deformation, Recrystallization; Precipitation**INTRODUCTION**

Al-Mg-Si alloys (EN AW 6xxx alloys) are structural hardening Aluminium alloys. They have notable overall properties with a good aptitude to hot deformation by rolling and cold drawing [1, 2]. The excellent mechanical and electrical properties of these alloys enabled their use in various sectors such as aerospace, automotive and transport of electricity [3-5]. The transition elements such as zirconium, chromium and manganese, which have low solubility and very slow diffusion rates in the  $\alpha$ -Aluminium solid solution, are generally added to EN AW 6xxx alloys to produce fine dispersoid particles. These fine particles dispersion retard the crystallization and increase the microstructure stability at high temperature due to their low solid solubility and diffusivity in Aluminium [6, 7]. It has been shown that the addition of transition elements to EN AW 6xxx alloys inhibit recrystallization when the alloys are pre-heated before deformation [8-10]. In EN AW 6xxx alloys, the nucleation of the dispersoid particles such as Zr-containing dispersoids, Mn-containing dispersoids, and Cr-containing dispersoids, which play the role of recrystallization inhibition, has been studied [11-15]. The needle-shaped Mn-containing dispersoids formed by using the rapid heating are much more effective than the fine spherical dispersoids formed by using the slow heating for grain refinement during the recrystallization process [16].

The grain growth and recrystallization will change the mechanical and chemical properties of the alloys. The information of the deformed state and annealing phenomena was detailed by Humphreys and Hatherly [17]. There is a succession of interesting processes for recrystallization dealing with the rearrangement of defects in the deformed crystals and conclude with the replacement of the deformed grain by a new set of strain-free crystals. The change in the recrystallization behaviour due to the presence of the second phase particles have been studied Sooner [18-20].

The cold rolling is a process that transforms the metal between two smooth or fluted rolls, rotating in the opposite direction. Due to this rotational movement and of the compression generated by the cylinders, there is a continuous reduction in the initial thickness by plastic deformation of the metal [1]. They are normally provided in planar shape whose width is dictated by that of the starting plate which they are cast, the length itself being limited by the constraints of transport. In recent years, the influence of cold rolling on the precipitation

processes in EN AW 6xxx alloys is widely studied [21-23]. It shows that the precipitation and growth of the second phase are accelerated significantly by this process. The larger grains have a preferred orientation (texture) when the alloy is more deformed [24, 25]. A study by Zhang [25] showed the effect of deformation and annealing on electrical conductivity, mechanical properties and texture of Al-Mg-Si alloy cables.

**EXPERIMENTAL PROCEDURE****Materials**

The Al-Mg-Si alloys were provided by Alcan International Limited of Canada. They were prepared by a direct chill casting process (DC) in a 178 mm of moulds. Then they were given a 10%, 20 %, 30%, 40% and 50% reduction in thickness by cold rolling in the air. The as-rolled alloys with the reduction in thickness of 50% (reduction in thickness) followed by an annealing for 1 h at different temperatures were chosen to study the effect of cold deformation on the microstructural changes and mechanical properties of as-rolled alloys. The chemical composition of the investigated alloys is given in Table 1. Alloy 1 contained at about 0.13wt. % Zr, while the alloy 2 was Zr-free and contained 0.65wt. % Mn. The as-cast specimens were heat-treated for 10 hours (h) at 550°C, cold-deformed by 10%, 20 %, 30%, 40% and 50% reduction in thickness and then annealed for 1 h at 350°C and 450°C and after that water quenched in order to follow the nucleation and growth of the dispersoids particles.

**Table 1** Chemical composition of the two alloys

Alloys	Si	Fe	Cu	Mn	Mg	Cr	Zr	Al
Alloy 1	0.6 2	0.21	0.42	0.006	1.01	0.002	0.13	ba 1
Alloy 2	1.3 0	0.23	0.004	0.65	0.79	0.001	-	ba 1

**Metallographic preparation**

Specimens for optical microscopy examination of each heat examination each heat treatment were mounted, ground on successive papers 180, 250, 350, 450, 600 and 800 and polished with 1-micron diameter diamond paste. They were finally polished on cloth with an alumina oxide particles suspension (OPS). The polished specimens were etched in Keller's reagent (1.5% HF - 2.5% HNO<sub>3</sub> - 95% water) for about 15 s.

Thin foils for TEM were prepared by spark machining to form discs 3 mm in diameter. The discs were subsequently grounded with fine silicon-carbide emery paper to about 200 mm thick. Final thinning was by jet polishing using a Struers Tenupol Unit with a solution of 33% HNO<sub>3</sub> in Analar grade methanol at -10 to -15 volts and a temperature of -20 to -30°C. When the electropolishing was completed the specimens were removed from the solution as quickly as possible and washed with Analar methanol. The specimens were dried between filter papers and then stored in a specimen grid box under vacuum.

**Optical microscopy**

Optical examination was carried out with an Olympus BH-2 microscope which contained a differential interference contrast (DIC) facility and polarised light.

**TEM microscopy**

Electron microscopy examination was carried out with an EM 300 electron microscope at 100 KeV. A liquid nitrogen-cooled decontaminator, an eccentric goniometer and double tilt holder were used to prevent the contamination after extended observation of an area of the thin foil.

**Hardness measurements**

Hardness measurements were performed using Vickers hardness tester. The test samples used for hardness measurements were 1x1 cm in size. Hardness data were determined with a load of 10 Kg (~ 98.06 N). Each measure of Vicker's hardness represents the mean value of at least 10 indentations

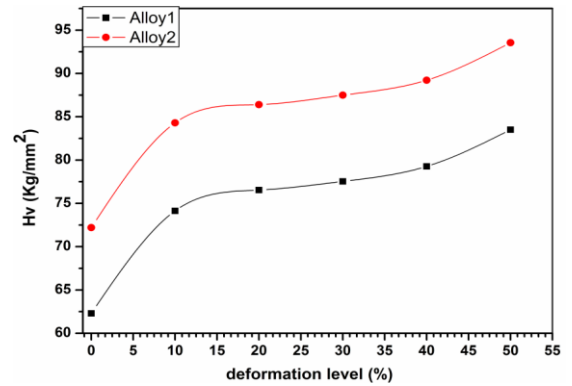
**RESULTS AND DISCUSSION**

Figure 1 shows the variation in microhardness as a function of different deformation level (0%, 10%, 20%, 30%, 40% and 50%) by cold rolling for the two alloys. An increase in microhardness is observed with the increase of the deformation level [5, 24, 26]. This increase in hardness is probably due to the high density of dislocations introduced by deformation of the two alloys by cold rolling, which leads to hardening of the alloys. This result confirms the results obtained by some researchers [5, 26].

The variation of the microhardness (HV) as a function of different deformation levels (0%, 10%, 20%, 30%, 40% and 50%) and then annealed for 1 h at 350°C and 450°C, and then water quenched of the two alloys is shown in Figure 2 and Figure 3.

The decrease in hardness is observed with the increasing of the annealing temperature in both alloys. This reduction in microhardness is attributed to the phenomenon of softening of the alloy pushed by the annealing treatment, which makes the increase in the ductility of the cold-rolled Al-Mg-Si alloy.

Figure 4 and Figure 5 show the optical micrographs of the two alloys in the cold deformed state and the microstructural change during the annealing of the cold-rolled solution treated alloys. Specimens of the two alloys are taken in the long-transverse direction.



**Fig. 1** Variation of microhardness as a function of deformation level of the two alloys

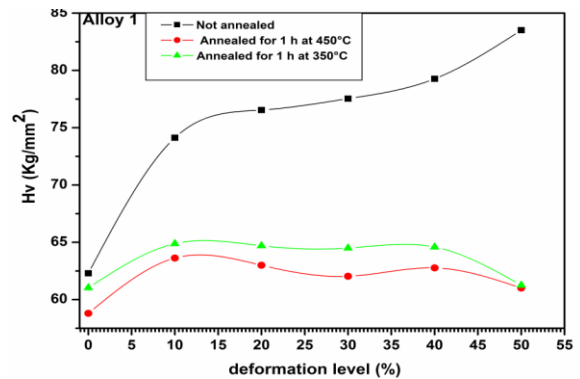


**Fig. 2** Variation of the microhardness (HV) as a function of the deformation level and then annealed for 1 h at 350°C and 450°C of alloy 1

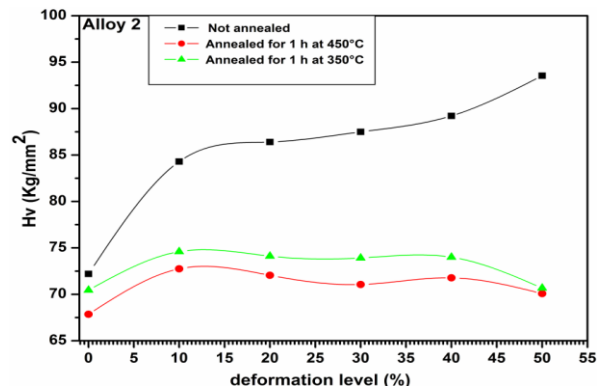


**Fig. 3** Variation of the microhardness (HV) as a function of the deformation level and then annealed for 1 h at 350°C and 450°C of alloy 2

The large grains can be seen to be strongly elongated in the rolling direction in the deformed state and after annealing up to 350°C. In a few areas, insoluble coarse particles originating from the cast structure appear to align themselves along the rolling direction. Alloy 1 shows only sub-structure inside the grains and less precipitate free zones along grain boundaries. Coarse particles were also observed elongated along the rolling direction. Some of them appear to be broken during the rolling. Optical micrographs revealed the sub-grain structure in the two alloys but more accentuate in the alloy 1. The main significant change in the microstructure was observed after annealing in the temperature 350°C.

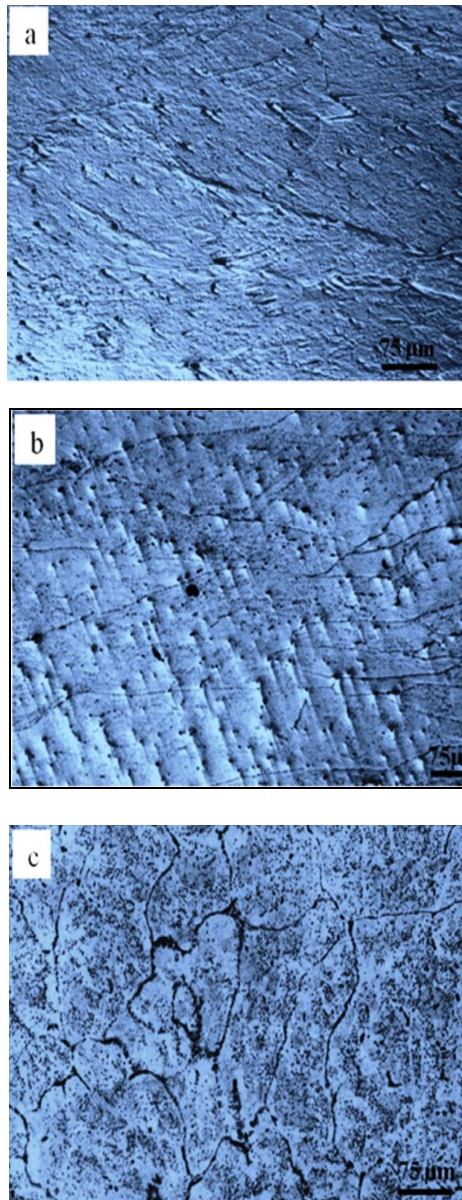


**Fig. 4** Optical micrographs of alloy 1 showing the microstructure change after rolling at room temperature to 50% reduction and annealing for 1 hour at: (a) as-rolled, (b) 350°C and (c) 450°C

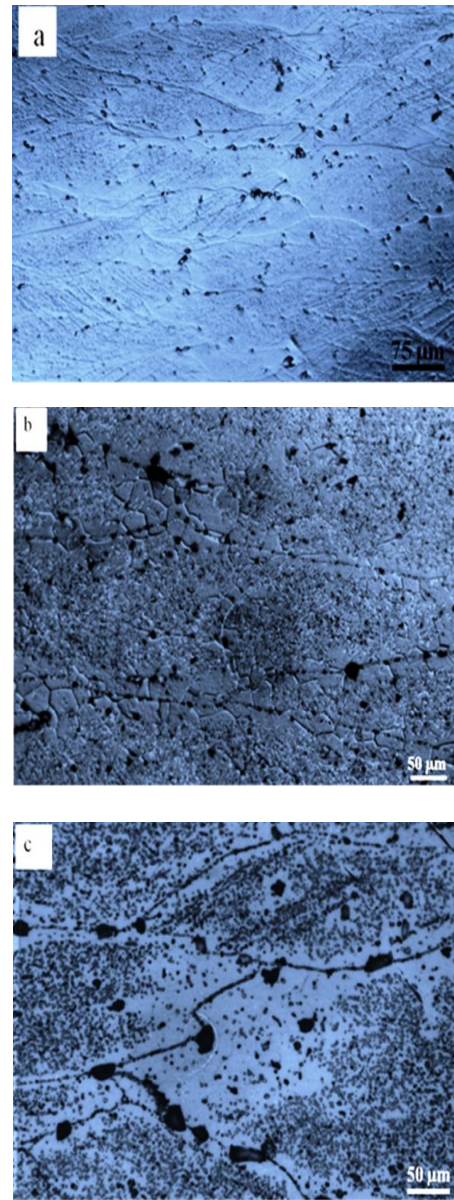


**Fig. 5** Optical micrographs of alloy 2 showing the microstructure change after rolling at room temperature to 50% reduction and annealing for 1 hour at: (a) as-rolled, (b) 350°C and (c) 450°C

Transmission electron micrographs in the longitudinal direction of the two alloys heat-treated for 10 h at 550°C and then cold deformed by 50% reduction in thickness and then annealed for 1 h at different temperatures are shown in Figure 6 and Figure 7.

After deformation, the microstructure of the two alloys are characterised by dislocation networks and well-defined cell structure, Figure 6a and Figure 7a. The co-existence of dispersoid particles and un-dissolved coarse particles is observed in the two alloys.

Coarse particles which mainly remain along grain boundaries are elongated along the rolling direction. Some of them look to be broken. Large particles generate a heterogeneous distribution of dislocations during deformation associated with a local high dislocation density at particle-matrix interfaces which could act as recrystallization nuclei during annealing. Electron microscopic observations show also that in all cases the coarse second phase particles were associated with a high dislocation density.

The dispersoid particles distribution is fairly homogeneous except in the regions around the coarse particles where the precipitate free zones (or PFZ's) were observed. Some coarse particles, with a particle size of about 2 to 3  $\mu\text{m}$ , give rise to a heavily local deformation of the Aluminium matrix. In the initial state cell interiors were filled with dislocations as well as sub-grain walls. Cleaning of cell interior and sharpening of cell boundaries were observed after an increase in ageing temperature. Hence sub-grain growth occurred; this result is in good agreement with the literature results [9, 10].

On annealing, well-defined sub-grains were formed (Figure 6b and Figure 7b) and at lower temperatures of annealing these were seen to grow by the migration of low angle boundaries at a rate controlled by the coarsening of the particles [18]. Most of the grain boundaries are not mainly straight but lie in contact with coarse particles. The irregular dislocation structure are replaced by a more regular fine-scale structure in which some cells begins to expand and serve as recrystallization nuclei. A good example of this phenomenon in aluminium has been found after very large rolling reductions (>95%), a stable fine-grained microstructure was formed on annealing, whereas at lower strains, normal discontinuous recrystallization occurred [18].

Fully recrystallized microstructure, Figure 6c and Figure 7c were achieved after annealing at 350°C for alloy 2 and 450°C for alloy 1.

Transmission electron micrographs revealed the precipitation of free silicon particles occurring during the recovery and recrystallization process. A mixed particle structure consisting of large coarse particles, resulting from the casting, and free silicon particles and dispersoid particles formed before deformation were also observed.

The dispersoid particles were not observed to be deformed after the cold deformation. PFZ's along the elongated grain and around the coarse particles were also observed. During the move of the sub-grain boundary, reacting with other dislocations will annihilate some dislocations, but the majority of them will enter the boundary. Hence the density of dislocations will increase.

The remaining coarse particles with a diameter greater than 2  $\mu\text{m}$  give rise to local deformation of the Aluminium matrix in their vicinity. This effect was more pronounced with a particle with a higher particle size.

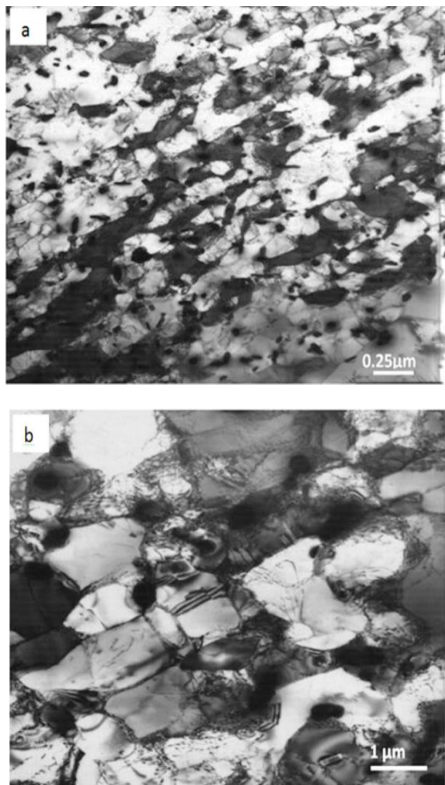


**Fig. 6** TEM of alloy 1 showing the microstructure change after rolling at room temperature to 50% reduction and annealing for 1 hour at (a) as-rolled, (b) 350°C and (c) 450°C

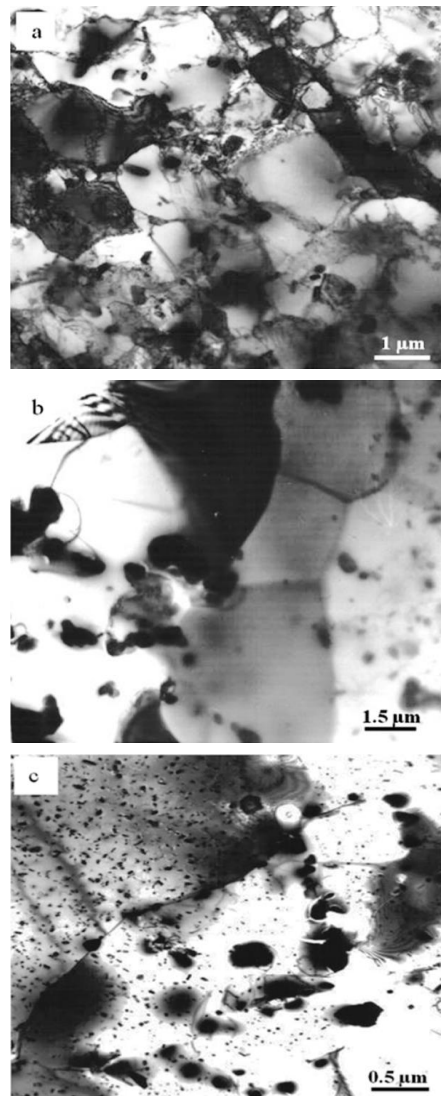
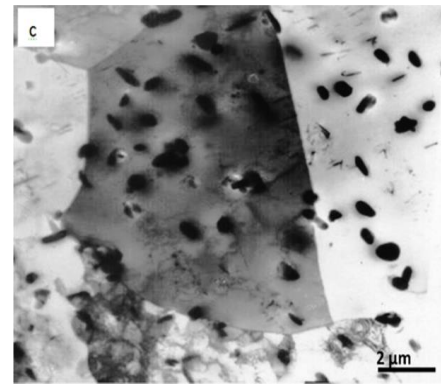


**Fig. 7** TEM of alloy 2 showing the microstructure change after rolling at room temperature to 50% reduction and annealing for 1 hour at (a) as-rolled, (b) 350°C and (c) 450°C

## CONCLUSIONS

Deformation by rolling Al-Mg-Si alloys causes an increase in microhardness and the annealing treatment decreases this microhardness, this increase in the microhardness due to the high density of dislocations introduced by deformation by cold rolling which accelerate the precipitation of the hardening phases. The structural change which occurs during the annealing is mainly due to the generation of sub-grains, from the elongated cell-structure, which was observed in the deformed matrix. Annealing at 350°C has little effect on the dislocation network. After a further increase in ageing temperature, the sub-grains grow by consuming the surrounding cell-structure; the dispersoid particles coarsen and become less effective in retarding recrystallization. The formation of a well-defined substructure due to the arrangement of dislocations is observed after the annealing temperature was increased. Large particles generate a heterogeneous distribution of dislocations during deformation associated with a local high dislocation density at particle-matrix interfaces, which could act as recrystallization nuclei during annealing.

**Acknowledgements:** Authors are grateful for the support of experimental works by research project (PRFU) under code number: B00L02UN120120190002 approved, on 01/01/2019, by the Ministry of Higher Education and Scientific Research in Algeria.

## REFERENCES

- H. Farh, T. Ziar, H. Belghit, M. Khechba, A. Noua, F. Serradj: Defect and Diffusion Forum, 397, 2019, 51. <http://dx.doi.org/10.4028/www.scientific.net/ddf.397.51>
- Y. Totik, R. Sadeler, I. Kaymaz, M. Gavkali: J. Mater. Process. Technol, 147, 2004, 60. <http://dx.doi.org/10.1016/j.jmatprotec.2003.10.026>
- T. Kvackaj, J. Bidulska, M. Fujda, R. Kocisko, I. Pokorny, O. Milkovic: Mater. Sci. Forum, 633-634, 2010, 273-302 <https://doi.org/10.4028/www.scientific.net/MSF.633-634.273>
- H. Belghit, H. Farh, T. Ziar, M. Zidani, M. Guemini: Arch. Metall. Mater, 63(4), 2018, 1643. <https://doi.org/10.24425/amm.2018.125088>
- M. Zidani, L. Bessais, H. Farh, M.D. Hadid, S. Messaoudi, D. Miroud, M.K. Loudjani, A.L. Helbert, T. Baudin: Steel Compos Struct, 22 (4), 2016, 745. <http://dx.doi.org/10.12989/scs.2016.22.4.745>
- Y. Wuhua, L. Zhenyu, Z.W. Chuanyang: Mater & Design, 34, 2012, 78. <https://dx.doi.org/10.1016/j.matdes.2011.07.003>
- Below: Mater. Sci. Forum, 217-222, 1996, 293. <http://dx.doi.org/10.4028/www.scientific.net/msf.217-222.293>
- T. Ziar, H. Farh, R. Guemini: Acta Metall Slovaca, 22(3), 2016, 138. <http://dx.doi.org/10.12776/ams.v22i3.697>
- R. Guemini, A. Boubertakh, G.W. Lorimer: J Alloy Compd, 486 (1-2), 2009, 451. <http://dx.doi.org/10.1016/j.jallcom.2009.06.207>
- H. Farh, R. Guemini : Appl. Phys. A-Mater, 119, 2015, 285. <http://dx.doi.org/10.1007/s00339-014-8963-5>
- P.J. Apps, M. Berta, P.B. Prangnell: Acta Mater, 53 (2), 2005, 499. <http://dx.doi.org/10.1016/j.actamat.2004.09.042>
- L. Lodgaard, N. Ryum: Mater. Sci. Eng A, 283, 2000, 144. [http://dx.doi.org/10.1016/s0921-5093\(00\)00734-6](http://dx.doi.org/10.1016/s0921-5093(00)00734-6)
- M. Cabibbo, E. Evangelista, C. Scalabroni, E. Bonetti: Mater. Sci. Forum, 503-504, 2006, 841. <http://dx.doi.org/10.4028/www.scientific.net/msf.503-504.841>
- H. Farh, K. Djemmal, R. Guemini, F. Serradj: Ann Chim-Sci Mat, 35(5), 2011, 283. <http://dx.doi.org/10.3166/acsm.35.283-289>
- D.H. Lee, J.H. Park S.W. Nam: Mat. Sci. Technol, 15(4), 1999, 450. <http://dx.doi.org/10.1179/026708399101505923>
- Y. Xu, H. Nagaumi, Y. Han, G. Zhang, T. Zhai: Metall. Mater Trans A, 48(3), 2017, 1355. <http://dx.doi.org/10.1007/s11661-016-3881-0>
- R. Hu, T. Ogura, H. Tezuka, T. Sato, Q. Liu: J. Mater. Sci. Technol, 26(3), 2010, 237. [http://dx.doi.org/10.1016/s1005-0302\(10\)60040-0](http://dx.doi.org/10.1016/s1005-0302(10)60040-0)
- F. Humphreys, M. Hatherly: Recrystallization and related annealing phenomena. Elsevier, Oxford, 2004. <http://dx.doi.org/10.1016/b978-008044164-1/50016-5>
- T. Ozawa: Bull. Chem. Soc. Japan, 38 (11), 1965, 1881. <http://dx.doi.org/10.1246/bcsj.38.1881>
- E.J. Mittemeijer: Recrystallization and Grain Growth. In: Fundamentals of Materials Science. Springer, Berlin, 2010. [http://dx.doi.org/10.1007/978-3-642-10500-5\\_10](http://dx.doi.org/10.1007/978-3-642-10500-5_10)
- V. Kumar, I.V. Singh, B. K Mishra: Acta Metall Sin, 27(2), 2014, 359. <http://dx.doi.org/10.1007/s40195-014-0057-z>
- H. L. Yu, A. K. Tieu, C. Lu, X.H. Liu, C. Kong: Mater Sci Eng A, 568, 2013, 212. <http://dx.doi.org/10.1016/j.msea.2013.01.048>
- B. Mirzakhani, Y. Payandeh : Mater Des, 68, 2015, 127. <http://dx.doi.org/10.1016/j.matdes.2014.12.011>
- H. Farh, R. Guemini, F. Serradj, K. Djemmal: Turk. J. Phys, 34(2), 2010, 117. Doi:10.3906/fiz-1004-27
- J. Zhang, M. Ma, F. Shen, D. Yi, B. Wang: Mater. Sci Eng A, 710, 2018, 27. <https://doi.org/10.1016/j.msea.2017.10.065>
- B. Wang, X. H Chen, F.S. Pan, J.J. Mao, Y. Fang: Trans. Nonferrous Met. Soc. China, 25, 2015, 2481. [https://doi.org/10.1016/S1003-6326\(15\)63866-3](https://doi.org/10.1016/S1003-6326(15)63866-3)